Eur. Phys. J. C (2023) 83:201
https://doi.org/10.1140/epjc/s10052-023-11364-7

THE EUROPEAN PHYSICAL JOURNAL C

Regular Article - Theoretical Physics

Do isotropic tidal forces imply isotropic cosmic expansion?

Fabio Scalco Dias[a], **Leandro Gustavo Gomes**[b], **Luis Fernando Mello**[c]

Institute of Mathematics and Computation, UNIFEI-Federal University of Itajubá, Av. BPS, 1303, Itajubá, Minas Gerais 37500-903, Brazil

Received: 20 December 2022 / Accepted: 25 February 2023

Abstract We investigate the dynamics of the spatially flat universes submitted to isotropic tidal forces and adiabatic expansion under Einstein's equations. Surprisingly, the tendency to a high Hubble anisotropy at late times starts to appear as far as we assume a strong-like energy condition to hold, a characteristic which becomes dominant in the radiation era and even more stringent under a stiff matter regime. This is a rather counter-intuitive behavior that shows us how, from the conceptual viewpoint, the Hubble parameter tends to anisotropize even when the universe is dominated by isotropic gravitational forces and usual physical conditions. We introduce the parameter b, which measures the relative variation in the magnitudes of the Hubble anisotropy against the scale factor, to show that mechanisms violating such an energy condition can compensate for this anisotropy increase. We also discuss if there is theoretical support for the existence of observational Hubble anisotropy in the late-time universe.

1 Introduction

Isotropy is quite an elusive property in Cosmology. The Hubble ratio of expansion was supposed to possibly vary no more than 1% along the different directions of the sky [1–4], the CMB data was thought to be independent of direction with a high degree of precision [5,6], and the number count of radio sources seemed to be consistent with the isotropy hypothesis [7]. Nonetheless, these assumptions have been put under further scrutiny along an increasing debate on their observational validity [8–10]. On the other side, from the theoretical point of view, the anisotropy in the Hubble parameter turns out to be unstable in the surroundings of the homogeneous universes [11], in general, which means that even small perturbations of it might increase to a magnitude far from the region where the universe could be considered isotropic. So, how far from isotropy does such magnitude evolve? Is it possible that we have arrived at an anisotropic late-time universe? In this manuscript, we tackle those questions in the spatially flat models going through an adiabatic expansion under the influence of isotropic tidal forces.

Historically, just after the discovery of the CMB in the '60 s, which by the time was showing its first traces of isotropy, the picture of a homogeneous, chaotic, and highly anisotropic early epoch had been proposed [12], often referred to as the BKL scenario. The current state of the universe would be achieved as the anisotropy dies out during the expansion, which could be caused by neutrino viscosity, for instance [13,14]. Soon after that, Collins and Hawking showed that the spatially homogeneous universes do not, in general, isotropize [11]. That was a distinguished point in the conceptual evidence for the instability of the Hubble isotropy in the FLRW models, which in turn became a barrier for the chaotic BKL picture [15]. Since then, the BKL approach survived as a general framework for approaching the big bang singularity [16], the dynamical aspects of the anisotropies have been further studied [17–21], and the inflationary theory came into the scene, leaving no "cosmic hair" neither in the form of homogeneity nor isotropy [22], and therefore giving theoretical support for the almost isotropic universe coming from our current observations.

Today, some decades after the results of Collins and Hawking, the behavior of the anisotropy under Einstein's dynamics can still baffle our intuition, even in the simplest of the models, under the most reasonable physical conditions. In order to show that, we start with a general spatially flat model, a Bianchi type I spacetime, which is put in an adiabatic expansion with only one restriction: the gravitational forces are everywhere isotropic so that the gravitational pull (or push) felt by the components of our free-falling cosmic fluid has

[a] e-mail: scalco@unifei.edu.br
[b] e-mail: lggomes@unifei.edu.br (corresponding author)
[c] e-mail: lfmelo@unifei.edu.br

Published online: 08 March 2023

no distinguished direction. As we are going to show, even under this framework favoring an isotropic behavior, the tendency to anisotropy still persists, and when the thermodynamic pressure is as high as in the case of pure radiation, it dominates completely. They form a class of simple and rather counter-intuitive examples, which enhances our understanding of the theoretical behavior of cosmic anisotropies. In particular, it displays a global nonlinear account of the anisotropy dynamics in a quite simple and physically reliable manner, which allows us to figure out how the tendency of isotropization/anisotropization varies with the equation of state of matter and how far this anisotropy can be located in order to occur one or other behavior.

This manuscript is about the conceptual understanding of the behavior of anisotropy in Cosmology. It has much more to add to our knowledge concerning issues involving the instability/stability of the Hubble isotropy, how far from the FLRW models, and under which kind of conditions, it might happen than to settle the behavior of its observational counterpart. It is divided as follows: in Sect. 2 we start with an exact example. Although it is not the model we will consider in the rest of the manuscript, it shows us the same qualitative aspects of the Hubble anisotropy parameter Σ that we will be facing later on. In Sect. 3, we define, in the context of the spatially flat models, what we mean by adiabatic expansion and by isotropy of the tidal forces. In the following section, we describe Einstein's equations in this setting, showing the first traces of the growth of the anisotropies. In the Sect. 5, we specialize the dynamics to those cases with a linear equation of state between the energy density and the thermodynamic pressure. This simplification gives us a whole class of examples where the global anisotropy dynamics can be seen in the Kasner disc, enlightening our understanding of such behaviors. In particular, we introduce a parameter b which measures the relative change in the magnitudes of the Hubble anisotropy and the scale factor. In Sect. 6, we analyze our findings in the face of recent observations and investigate whether they can support the idea of an observable Hubble anisotropy in the late-time universe. In the final section, we make our concluding considerations. The notations and sign conventions follow the reference [23].

2 Hubble anisotropy vs isotropic tidal forces: an exact solution

Before we start our main investigation, let us make a detour and consider an exact model that contains a simple example by assuming that the tidal forces act as an isotropic "elastic medium", so that the geodesic deviation equation turns into

$$\frac{d^2\xi^i}{dt^2} = -\,\mathrm{R}^i_{0k0}\,\xi^k = -\kappa\,\xi^i, \tag{1}$$

with κ constant. For the diagonal Bianchi-I metric [23] $(\mathrm{g}_{ij}) = \mathbf{diag}\{-1, a_1(t), a_2(t), a_3(t)\}$, this condition means that

$$\ddot{a}_i = -\kappa\, a_i, \quad a_i(0) = 1, \quad \dot{a}_i(0) = \mathrm{H}_{0i}, \tag{2}$$

where we have set $t_0 = 0$ for "today", the isotropic initial conditions $a_1(0) = a_2(0) = a_3(0) = 1$ for the metric and the Hubble constant in each principal space direction as $\mathrm{H}_i(0) = \mathrm{H}_{0i}$. The expansion and the Hubble anisotropy tensors are also diagonal, $(\theta^i_j) = \mathbf{diag}\{\mathrm{H}_1, \mathrm{H}_2, \mathrm{H}_3\}$ and $(\Sigma^i_j) = \mathbf{diag}\{\Sigma_1, \Sigma_2, \Sigma_3\}$, respectively, where

$$\mathrm{H}_i = \frac{\dot{a}_i}{a_i} \quad \text{and} \quad \Sigma_i = \frac{\mathrm{H}_i - \mathrm{H}}{\sqrt{6}\,\mathrm{H}}, \tag{3}$$

with $\mathrm{H} = (\mathrm{H}_1 + \mathrm{H}_2 + \mathrm{H}_3)/3$, the Hubble parameter. The factor "$\sqrt{6}$" is chosen in order to put $\Sigma = 1$ as an important benchmark, setting the boundary between intermediate ($\Sigma < 1$) and extreme ($\Sigma > 1$) anisotropies [21]. The Hubble anisotropy magnitude is defined as

$$\Sigma = \sqrt{(\Sigma_1)^2 + (\Sigma_2)^2 + (\Sigma_3)^2}. \tag{4}$$

As we solve the initial value problem (2) and define $\omega_0 = \sqrt{|\,\kappa\,|}$, we arrive to $\mathrm{H}_i = \mathrm{H}_{0i}$, for $\kappa = 0$, and

$$\frac{\mathrm{H}_i}{\omega_0} = \begin{cases} \frac{\mathrm{H}_{0i} + \omega_0\,\tanh(\omega_0 t)}{\omega_0 + \mathrm{H}_{0i}\,\tanh(\omega_0 t)}, & \kappa < 0, \\ \frac{\mathrm{H}_{0i} - \omega_0\,\tan(\omega_0 t)}{\omega_0 + \mathrm{H}_{0i}\,\tan(\omega_0 t)}, & \kappa > 0. \end{cases} \tag{5}$$

Note that the constant κ is, in fact, $(\rho + 3\mathrm{P})/6$, where ρ and P are the energy density and pressure of the energy-momentum tensor (see Eq. (9) below). Hence, the condition $\rho < -3\mathrm{P}$ is equivalent to $\kappa < 0$, which resembles the violation of the strong energy condition. In this case, nothing unusual appears: the anisotropy decays exponentially with time, in a way very similar to the cosmic non-hair theorem [22]. As we re-write the solution above in the form

$$\mathrm{H}_i = \omega_0 + \frac{2\omega_0(\mathrm{H}_{0i} - \omega_0)\, e^{-2\omega_0 t}}{\mathrm{H}_{0i} + \omega_0 - (\mathrm{H}_{0i} - \omega_0)\, e^{-2\omega_0 t}}, \tag{6}$$

we clearly see that $\mathrm{H}_i \to \omega_0$ exponentially as t increases, that is, $\Sigma \to 0$ exponentially in time.

On the other hand, as $\rho > -3\mathrm{P}$ ($\kappa > 0$) and the initial expansion ratios are positive, $\mathrm{H}_{0i} > 0$ for $i = 1, 2, 3$, with regular initial Hubble anisotropy $\Sigma(0) < 1/2$, we note from the last of the formulas in (5) that, at some finite time T, we have different signs of the Hubble ratios along two different directions, say, for instance, $\mathrm{H}_1(T) < 0$ while $\mathrm{H}_2(T) > 0$. This fact can happen only in the region $\Sigma > 1/2$ [21]. Therefore, we conclude that the Hubble anisotropy must increase at some point, no matter how small $\Sigma(0) > 0$. Indeed, our numerical simulation in Fig. 1 tells us that Σ explodes at a finite time. This should be quite expected, for this model contains a restoring elastic force. At some point, the mean expansion is halted, when $\mathrm{H} = 0$, and starts the contraction

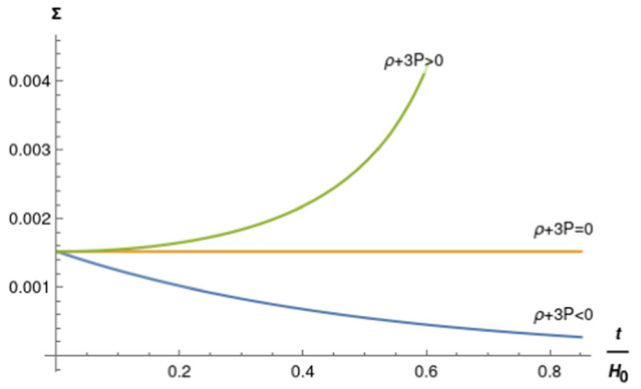

Fig. 1 The future evolution of the Hubble anisotropy $\Sigma(t)$ in the case of elastic tidal forces with $\omega_0 = \mathrm{H}_0$, $\mathrm{H}_{01}/\mathrm{H}_0 = 1.001$, $\mathrm{H}_{02}/\mathrm{H}_0 = 1.002$ and $\mathrm{H}_{03}/\mathrm{H}_0 = 0.997$. For $\rho < -3\mathrm{P}$, the anisotropy decreases with time. For $\rho > -3\mathrm{P}$, it increases

phase. Since this will not occur simultaneously along all the spatial directions, there will be at least one of the H_i's not vanishing, which implies the blow-up of the ratio H_i/H, and so does Σ.

In this manuscript, we will investigate a different system, where the universe is ever-expanding in an adiabatic way and matter has a quite usual behavior (see Eq. (22), for instance). Contrary to the elastic model, the Hubble parameter does not vanish at a finite time, so that Σ does not blow up. Nonetheless, we observe the same phenomena occurring in both models: starting somewhere around the condition $\rho = -3\mathrm{P}$, the anisotropy starts changing its behavior, so that the tendency of anisotropization, instead of isotropization, starts to overtake the entire system as far as ρ gets greater than $-3\mathrm{P}$. This evolution, parametrized by the ratio $\mathrm{w} = \mathrm{P}_T/\rho$, P_T the pressure in thermodynamic equilibrium (see Sect. 3), is shown through the figures Figs. 2, 3, 4, 5 and 6. Therefore, we observe that even when the gravitational forces are kept isotropic, the tendency of a growing anisotropy surrounds the FLRW models, where $\Sigma = 0$. In accordance with the picture of cosmology most accepted nowadays, the anisotropies must represent only tiny corrections to the FLRW models. Hence, we introduce the parameter b (Eq. (27)) which helps us understand how the alternating periods of isotropization and anisotropization could lead to an almost isotropic universe.

3 Isotropy of the tidal forces and adiabatic expansion in spatially flat universes

Our main assumption is that the universe allows a class of free-falling observers to whom the space sections are flat and the tidal forces are isotropic. This means that the gravitational forces should balance out in a way that the pull (or push) felt by any of these observers is the same in any direction. As we put this forward in the mathematical language, the observers are represented by a unitary, geodesic, and vorticity-free fundamental velocity, u, whose space sections are flat, that is, a Bianchi type I model, in a way the tidal force operator, $-\mathrm{R}^{\mu}_{\kappa\nu\lambda}\mathrm{u}^{\kappa}\mathrm{u}^{\lambda}$, has no preferred spatial directions. This means that it is a multiple of the identity along the spatial directions, which is equivalent to the equation of state ([23], sec. 6.4)

$$E^{\mu}_{\nu} = \tfrac{1}{2}\,\Pi^{\mu}_{\nu}, \tag{7}$$

where E^{μ}_{ν} is the electric part of the Weyl tensor and Π^{μ}_{ν} the anisotropic stress tensor. In this case, as we use adapted coordinates (t, x^i) for which $\mathrm{u} = \partial_t$, the metric is

$$\mathrm{g} = -dt^2 + \mathrm{h}_{ij}(t)\,dx^i\,dx^j. \tag{8}$$

The geodesic deviation equations along the spatial directions turn into ([23], sec. 6.4)

$$\frac{d^2\xi^i}{dt^2} = -\frac{1}{6}\,(\rho + 3\,\mathrm{P})\,\xi^i, \tag{9}$$

where $\rho = T_{\mu\nu}\mathrm{u}^{\mu}\mathrm{u}^{\nu}$ and $\mathrm{P} = T^i_i/3$ stand for the energy density and total pressure, respectively. The Hubble and the matter-radiation anisotropies will be identified with the dimensionless spatial tensors [21] $\Sigma^j_i = \sigma^j_i/(\sqrt{6}\,\mathrm{H})$ and $\mathcal{N}^j_i = \Pi^j_i/(\sqrt{6}\,\mathrm{P})$, respectively, where σ^j_i is the shear tensor and Π^j_i the anisotropic stress tensor. Hence, the electric part of the Weyl tensor becomes ([23], exercise 6.4.1)

$$\frac{1}{\sqrt{6}}\,E^i_k = \mathrm{H}^2\,\Sigma^i_k - \frac{1}{2}\,\mathrm{P}\,\mathcal{N}^i_k - \sqrt{6}\,\mathrm{H}^2\left(\Sigma^i_{\ell}\Sigma^{\ell}_k - \frac{\Sigma^2}{3}\,\delta^i_k\right), \tag{10}$$

where $\Sigma = \sqrt{\Sigma^i_k\Sigma^k_i}$ is the Hubble anisotropy magnitude. Finally, we can re-write the equation of state (7) as

$$\mathrm{P}\,\mathcal{N}^i_k = \mathrm{H}^2\left(\Sigma^i_k - \sqrt{6}\left(\Sigma^i_{\ell}\Sigma^{\ell}_k - \tfrac{\Sigma^2}{3}\,\delta^i_k\right)\right). \tag{11}$$

We assume an adiabatic expansion, with no energy flux, $q^i = 0$, nor any spatial heat diffusion, $\partial_i T = 0$, so that the entropy is conserved: $\dot{S} = 0$. As we split the pressure in its bulk and thermodynamic counterparts, P_B and P_T, respectively, we obtain ([23], sec. 5.2)

$$\frac{dS}{dt} = 0 \Rightarrow \mathrm{P}_B = \mathrm{P} - \mathrm{P}_T = -2\,\mathrm{P}\,\mathcal{N}_{ik}\,\Sigma^{ik}. \tag{12}$$

This means that the bulk pressure is composed by the Hubble and matter-radiation components of the anisotropy. On the other hand, the energy conservation, $\nabla_{\mu}\,T^{\mu}_0 = 0$, turns out to be dependent only on the pressure in thermodynamic equilibrium, since it is written as ([23], sec. 5.1)

$$\frac{d\rho}{dt} = -3\mathrm{H}\,(\rho + \mathrm{P}_T). \tag{13}$$

It is worth mentioning that this equation emulates the conservation of energy in the FLRW spacetimes. Therefore, P_T should be interpreted as the "isotropic" part of the total pressure, which is responsible for the net force the cosmic fluid

exerts upon the fabric of the spacetime. On the other hand, P_B accommodates that part remaining in the process of taking thermodynamical averages, no less important.

4 The cosmic dynamics from Einstein's equations

The Einstein's equations in the variables Σ^i_k and $\mathcal{N}^i_k$ have been put forward in Ref. [21]. They are equivalent to the Generalized Friedmann equation,

$$\rho = 3\left(1-\Sigma^2\right)\mathrm{H}^2, \tag{14}$$

where $\Sigma = \sqrt{\Sigma^i_k\Sigma^k_i}$ is the Hubble anisotropy magnitude, the conservation of energy (13) and the anisotropy equation, which after applying the condition (11) for isotropic tides, becomes

$$\frac{1}{\mathrm{H}}\frac{d}{dt}\Sigma^i_k = \left(1-\frac{\rho-\mathrm{P}}{2\,\mathrm{H}^2}\right)\Sigma^i_k - \sqrt{6}\left(\Sigma^i_\ell\Sigma^\ell_k - \frac{\Sigma^2}{3}\,\delta^i_k\right). \tag{15}$$

The first consequence of the tidal anisotropy is that the relation (11) allows Σ^i_k and $\mathcal{N}^i_k$ to be simultaneously diagonalizable, and hence, as we put $\Sigma^i_k(t_0)$ in the diagonal form, the Einstein's equations tell us that it will continue to be like that along the entire expansion. In other words, our Bianchi I spacetime is diagonalizable.[1] Hence, the system (15) is completely determined by the equations for the Hubble anisotropy magnitude Σ and the Kasner angle α, as

$$(\Sigma^k_i) = \sqrt{\frac{2}{3}}\,\Sigma\begin{bmatrix}\sin\alpha & 0 & 0\\ 0 & \sin\left(\alpha+\frac{2}{3}\pi\right) & 0\\ 0 & 0 & \sin\left(\alpha-\frac{2}{3}\pi\right)\end{bmatrix}. \tag{16}$$

From this and the relation (11), we can write the bulk pressure as

$$\mathrm{P}_B = -\,2\,\Sigma^2\,\mathrm{H}^2\,\left(1+\Sigma\,\sin(3\alpha)\right). \tag{17}$$

By using the new time parameter $ds = \mathrm{H}dt$ and the "equation-of-state" variable w, that is,

$$s(t) = \ln\left(\frac{a(t)}{a_0}\right) \quad \text{and} \quad \mathrm{w}(t) = \frac{\mathrm{P}_T(t)}{\rho(t)}, \tag{18}$$

the energy conservation becomes

$$\rho' = -3(\mathrm{w}+1)\,\rho, \tag{19}$$

while the anisotropy equation turns into

$$\begin{cases}\Sigma' = \Sigma\left(1-\Sigma^2\right)\left(\Sigma\,\sin(3\alpha)+\dfrac{3\mathrm{w}-1}{2}\right),\\ \alpha' = \Sigma\,\cos(3\alpha),\end{cases} \tag{20}$$

where we have used the abreviation $z' = dz/ds$. We will consider only the inner part of the Kasner disc ($\Sigma \le 1$), since this is equivalent of keeping the energy density non-negative, according to the generalized Friedmann equation (14).

5 The cosmic dynamics for fluids with a linear equation of state

In order to have a glimpse of the different features of the dynamical behavior of our cosmic system, we will consider the expansion with w constant, that is, with the energy density and the pressure in thermodynamic equilibrium satisfying the linear equation of state $\rho = \mathrm{w}\,\mathrm{P}_T$, with $\mathrm{w}' = 0$.

5.1 General properties of the solutions

Equations (20) define a smooth and autonomous system in the Kasner disc $\Sigma \le 1$. In the "Cartesian" coordinates, $x = \Sigma\,\cos(3\alpha)$ and $y = \Sigma\,\sin(3\alpha)$, it turns out to be polynomial, as

$$\begin{cases}x' = x\left(1-x^2-y^2\right)\left(y+\dfrac{3\mathrm{w}-1}{2}\right) - 3xy,\\ y' = y\left(1-x^2-y^2\right)\left(y+\dfrac{3\mathrm{w}-1}{2}\right) + 3x^2.\end{cases} \tag{21}$$

Since all the solutions are kept inside the compact disc, they are defined for every real value of s, that is, for every $a > 0$. Hence, for all of them, as we assume expansion ($\dot{a} > 0$), we have two distinct epochs, just as in the FLRW case: the early ($a \ll a_0$) and the late-time ($a \gg a_0$) universes. Furthermore, the conservation (19) is also analogous to its counterpart in the isotropic universes, so that the energy density turns out to be

$$\rho(t) = \rho_0\left(\frac{a_0}{a(t)}\right)^{3(\mathrm{w}+1)}. \tag{22}$$

The anisotropy magnitude Σ and the Kasner angle α, in general, cannot be fully integrated from the equations in (20). Notwithstanding, as we observe that

$$\frac{d\Sigma}{\Sigma(1-\Sigma^2)} = \tan(3\alpha)d\alpha + \frac{3\mathrm{w}-1}{2}\frac{da}{a} \tag{23}$$

whenever $\cos(3\alpha_0) \neq 0$, we obtain the constraint

$$\Sigma(t) = \frac{\Sigma_0}{\sqrt{\Sigma_0^2 + (1-\Sigma_0^2)\xi(t)}} \tag{24}$$

with

$$\xi(t) = \left(\frac{a_0}{a(t)}\right)^{3\mathrm{w}-1}\left(\frac{\cos(3\alpha(t))}{\cos(3\alpha_0)}\right)^{\frac{2}{3}}. \tag{25}$$

On the other hand, the solutions with $\sin(3\alpha_0) = \pm 1$ satisfy $\alpha' = 0$. Hence, by a direct integration of the first of the

[1] In general, a Bianchi I spacetime is not diagonalizable. See the appendix in [19].

equations in (20), we obtain

$$\int_{\Sigma_0}^{\Sigma(t)} \frac{d\Sigma}{\Sigma\left(1-\Sigma^2\right)\left(\frac{3w-1}{2}\pm\Sigma\right)} = \ln\left(\frac{a(t)}{a_0}\right). \tag{26}$$

Note that in the generic case (24), when $w > 1/3$, as we set $a \to \infty$ we get $\xi \to 0$ and $\Sigma \to 1$. This implies that these solutions get more and more anisotropic as the universe expands. This rather counter-intuitive behavior, since the tides are kept isotropic, persists even when w attains smaller values, up to the breaking point of the strong energy condition, $w = -1/3$. This important fact will be addressed throughout the text.

It is interesting to analyze the relation of the orders of magnitude both the scale factor and the anisotropy went through between two specific moments of the expansion of the universe, say from t_1 to t_2. This is characterized by the parameter

$$b = \left\| \frac{\ln(\Sigma_2/\Sigma_1)}{\ln(a_2/a_1)} \right\|. \tag{27}$$

As we analyze it along the solutions $\sin(3\alpha_0) = \pm 1$, we have, according to (26),

$$\frac{1}{b} = \left\| \frac{1}{\ln(\Sigma_2/\Sigma_1)} \int_{\Sigma_1}^{\Sigma_2} \frac{d\Sigma}{\Sigma\left(1-\Sigma^2\right)\left(\Sigma\pm\frac{3w-1}{2}\right)} \right\|. \tag{28}$$

As we take $\Sigma_2/\Sigma_1 \to 0$ or $\Sigma_1/\Sigma_2 \to 0$ in (28), we conclude that

$$b \approx \frac{|3w-1|}{2} \tag{29}$$

whenever one of the variables Σ_1 or Σ_2 overcomes the other in many orders of magnitude. These formulas will be of suitable usage in order to estimate the variation of the anisotropy magnitudes during the different epochs of the universe.

5.2 The qualitative aspects of the dynamics

The equilibrium points of the system (20), with w constant, are the origin, $\Sigma = 0$, representing the flat FLRW universe, the Taub points in the Kasner circle $\Sigma = 1$, and the LRS points inside the disc,[2] with $\Sigma = |3w-1|/2$. They come in two categories: the T's and the Q's. The Taub points T_1, T_2, T_3, with $\Sigma = 1$, and the LRS ones $\widetilde{T}_1$, $\widetilde{T}_2$, $\widetilde{T}_3$, with $\Sigma = (3w-1)/2$, these last ones existing only in the case $1/3 \le w \le 1$, have the following Kasner angles coordinates, respectively,

$$\alpha_1 = \frac{\pi}{2}, \quad \alpha_2 = \frac{11\pi}{6}, \quad \alpha_3 = \frac{7\pi}{6}.$$

[2] For the Taub points, see [20]. Any point with Kasner angular coordinates $n\pi/6$, n odd, is Locally Rotationally Symmetric (LRS), which refers to the more symmetric configuration of the spacetime. A good analogy is to compare the ellipsoids of revolution in the Euclidean spaces (LRS) with their less symmetric partners.

Table 1 Topological type of each equilibrium point of system (20) for $-1 \le w \le 1$

w/point	Origin	Q_i	T_i	$\widetilde{Q}_i$	$\widetilde{T}_i$
$w \in [-1, -1/3)$	SN	S	UN	$\nexists$	$\nexists$
$w = -1/3$	SN	S-N	UN	Q_i	$\nexists$
$w \in (-1/3, 1/3)$	SN	SN	UN	S	$\nexists$
$w = 1/3$	6 HS	SN	UN	Origin	Origin
$w \in (1/3, 1)$	UN	SN	UN	$\nexists$	S
$w = 1$	UN	SN	S-N	$\nexists$	T_i

The Taub points Q_1, Q_2, Q_3, with $\Sigma = 1$, and the LRS ones $\widetilde{Q}_1$, $\widetilde{Q}_2$, $\widetilde{Q}_3$, with $\Sigma = (1-3w)/2$, these last ones existing only in the case $-1 \le w \le 1/3$, have the following Kasner angles coordinates, respectively,

$$\alpha_1 = \frac{3\pi}{2}, \quad \alpha_2 = \frac{5\pi}{6}, \quad \alpha_3 = \frac{\pi}{6}.$$

Note that when $w = -1/3$, the points $\widetilde{Q}_i$'s coincide with the Q_i's, and when $w = 1$, the points $\widetilde{T}_i$'s coincide with the T_i's. Moreover, as $w \to 1/3^+$, $\widetilde{T}_i$ approach the origin, as well as $\widetilde{Q}_i$, when $w \to 1/3^-$.

The linear part of system (21) at the origin is

$$\begin{bmatrix} (3w-1)/2 & 0 \\ 0 & (3w-1)/2 \end{bmatrix}. \tag{30}$$

At the Taub points, the linear part of system (20) is

$$\begin{bmatrix} 3-3w & 0 \\ 0 & 3 \end{bmatrix} \quad \text{or} \quad \begin{bmatrix} -(3w+1) & 0 \\ 0 & -3 \end{bmatrix}, \tag{31}$$

whether the point is T_i or Q_i ($i = 1, 2, 3$), respectively. Finally, for the points $\widetilde{T}$'s or $\widetilde{Q}$'s, we obtain

$$\begin{bmatrix} \frac{3}{8}(9w^2-1)(w-1) & 0 \\ 0 & \frac{3}{2}(3w-1)) \end{bmatrix}. \tag{32}$$

In short, the stability of each of these points is given in Table 1 where the following notation is used: S (saddle), UN (unstable node), SN (stable node) HS (hyperbolic sectors) and S-N (saddle-node) [24].

In what follows, we analyze the dynamics in the Kasner disc ($\Sigma \le 1$) with the variables Σ and α working as "polar coordinates" in the plane [20,21]. We are interested in the interval $-1 \le w \le 1$. We could abuse of our intuition and refer to the condition $w = 0$ as "dust", $w = 1/3$ as "radiation", $w = 1$ as "stiff-matter", and so on. This would be justified as far as the anisotropies are kept small, so that we could interpret those situations as small perturbations of the proposed physical situation. In the case the anisotropies grow large, those proposed names could be quite misleading. For this reason, we will adopt the names "dust-like", "radiation-like", "stiff-matter-like", and so on. In particular, for $w = -1$, both ρ and P_T are constant, according to the

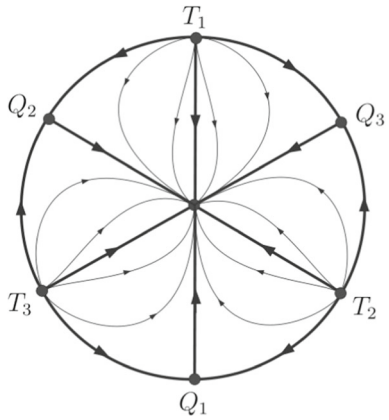

Fig. 2 The phase portrait in the Kasner disc ($\Sigma \leq 1$) for $-1 \leq \mathrm{w} \leq -1/3$. Any solution isotropizes towards the FLRW universe at the center. The T-Taub points are unstable nodes. The Q-Taub points are saddles up to the value $\mathrm{w} = -1/3$, when they coincide with the $\widetilde{Q}$'s and begin the transition to stable nodes. In this case, they are saddle-nodes

conservation equation (13). Hence, we shall refer to this situation as Λ-like, since it is equivalent to the introduction of the cosmological constant Λ.

5.2.1 *From the Λ-like scenario to the breaking point of the strong energy condition*

According to the standard picture of Cosmology, the interval $-1 \leq \mathrm{w} < -1/3$ encompass the very early inflationary era as well as the late-time dark energy period, both satisfying $\mathrm{P}_T \approx -\rho$. The state $\mathrm{w} = -1/3$ will be referred to as the breaking point of the strong energy condition.[3] Here, the T-Taub points are unstable nodes while the Q's are saddles, with all the solutions inside the Kasner disc converging to the late-time isotropic cosmology, that is, $\Sigma \to 0$ as $a \to \infty$ (see Fig. 2).

Since the anisotropy decreases as the universe expands, let us pick the initial and final states, Σ_1 and Σ_2, respectively, with $\Sigma_2 \ll \Sigma_1$. According to the formula (29), we have $b \approx (1-3\mathrm{w})/2$. This means that the anisotropy diminishes twice as fast as the universe expands, if $\mathrm{w} = -1$, or at the same ratio, if $\mathrm{w} = -1/3$. Let us analyze the first case separately, due to its conceptual importance.

The parameter b in the case $\mathrm{w} = -1$ can be straightforwardly calculated through the integral (28) along the solution $\alpha = \pi/2$. If we take $\Sigma_2 = \Sigma_1 \times 10^{-n}$, $n > 1$, we obtain

$$\frac{2}{b} - 1 \approx \frac{-\ln(1-\Sigma_1) + \ln(1+\Sigma_1/2) - 2\ln(1+\Sigma_1)}{3n \ln 10}, \tag{33}$$

[3] Indeed, the strong energy condition demands $\rho + 3\mathrm{P} > 0$ and $\rho + \mathrm{P} + \Pi_i > 0$, $i = 1, 2, 3$, Π_i the eigenvalues of Π_{ij}. The name refers to the state at which it begins to be violated, at least for small anisotropy ($\Sigma \approx 0$).

where we have used $\ln(1 + \Sigma_1 \times 10^{-n}) \approx 0$. For Σ_1 not too close to 1, we have $b \approx 2$, just as aforementioned. On the other hand, if the initial condition was extremely anisotropic, as $\Sigma_1 = 1 - 10^{-n_1}$, we would have $b \approx 2 - 2n_1/(3n + n_1)$, meaning that b could attain smaller values, but we would still have $b \geq 4/3$. Hence, when $\mathrm{P}_T = -\rho$, the anisotropy vanishes faster than the universe expands. Furthermore, if the universe has passed through N e-folds during this period, the anisotropy would diminish something near to $2N$ e-orders of magnitude. This is in agreement with the no-hair picture of the cosmic evolution [22]. As we apply it to the inflationary period, where the universe is believed to have stayed long enough as $N \gtrsim 60$ with a predominant equation of state $\mathrm{w} = -1$ [23], we would have the anisotropy at the beginning of the reheating period probably as tiny as $\Sigma_{rh} \lesssim e^{-120}$. If not that, at least it would not be greater than e^{-80}, as we put $b = 4/3$. An analogous situation would occur during the late-time dominance of the dark energy, but now with an inferior value for N.

5.2.2 *From the breaking point of the strong energy condition to the radiation-like condition*

From the dynamical viewpoint, the interval $-1/3 \leq \mathrm{w} < 1/3$ is characterized by the origin still being a stable node, but at this time its basin of attraction is not the inner Kasner disc anymore. In fact, new saddle-type equilibrium points appear along the straight segments connecting the Q-Taub points to the origin, those LRS ones labeled as $\widetilde{Q}_1$, $\widetilde{Q}_2$ and $\widetilde{Q}_3$. To each of them, there correspond two separatrices splitting the disc into two parts: the inner one, which contains the basin of attraction for the equilibrium at the origin, where the universe tends to a late-time isotropic state, and the outermost one, where the anisotropization takes place, and the solutions tend to the highly anisotropic LRS universes at the Q-Taub points.

The $\widetilde{Q}$'s equilibrium points at $\Sigma = (1 - 3\mathrm{w})/2$ split the line $\alpha = (1 + 4n)\pi/6$ in two: the isotropization and anisotropization segments, where $0 < \Sigma < (1 - 3\mathrm{w})/2$ and $(1 - 3\mathrm{w})/2 < \Sigma < 1$, respectively (see Fig. 3).As we estimate the order of magnitude parameter b with the aid of the formula (29), we obtain

$$\Sigma_2 \ll \Sigma_1 < \frac{1-3\mathrm{w}}{2} \quad \Rightarrow \quad b = \frac{1-3\mathrm{w}}{2}. \tag{34}$$

Therefore, as $\Sigma_1 < \frac{1-3\mathrm{w}}{2}$, the anisotropy decays slower than the universe expands, by a factor b, with $0 < b < 1$, such that $b \to 1$ as $\mathrm{w} \to -1/3^+$ and $b \to 0$ as $\mathrm{w} \to 1/3^-$. In the case of dust-like solutions ($\mathrm{w} = 0$), we have that every two e-folds of the universe corresponds to one of the anisotropy, such that $b = 1/2$, as long as $\Sigma_1 < 1/2$. On the other hand, when $\Sigma_1 > \frac{1-3\mathrm{w}}{2}$, the parameter b loses its general character so that the estimate it is intended for should

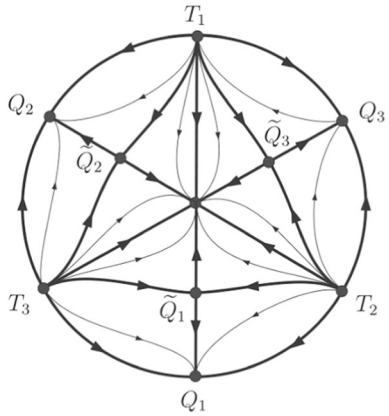

Fig. 3 The phase portrait in the Kasner disc ($\Sigma \leq 1$) for $-1/3 < \mathrm{w} < 1/3$. There are separatrices splitting the dynamics in two main global behaviors. In the innermost part, the solutions isotropize towards the FLRW universe at late times. In the outermost one, the universes tend to the highly anisotropic LRS models at the Q-Taub points. As we get closer to the radiation epoch ($\mathrm{w} \to 1/3^-$), anisotropization starts to dominate over isotropization

be directly calculated from the integral (28), since it can give any positive number.

5.2.3 The radiation-like era

The radiation-like era is distinguished as being the transition point to pure anisotropization. In fact, the $\widetilde{Q}$-type equilibrium points coalesce with the origin, so that the anisotropization sector becomes virtually the only one available inside the Kasner disc, except for the segments where $\sin(3\alpha_0) = -1$, the remains of the former isotropization region. Therefore, the isotropic universe is no longer stable for small perturbations, for $\Sigma \to 1$ as $a \to \infty$, no matter the initial values as far as we keep $\Sigma_0 \neq 0$ and $\sin(3\alpha_0) \neq -1$. The special cases where $\sin(3\alpha_0) = -1$ are still tending to the late-time FLRW model. The dynamics in the Kasner disc for this epoch is depicted in Fig. 4.

In the case $\cos(3\alpha_0) \neq 0$, we obtain from the formula (24) the first integral

$$\frac{(1-\Sigma^2)^{3/2}}{\Sigma^3 \cos(3\alpha)} = c_0. \tag{35}$$

This implies that system (20) is integrable for $\mathrm{w} = 1/3$.

Let us assume that our model describes the hot and dense epoch dominated by radiation when the input anisotropy was Σ_1, and by the end of this period, when the CMB was released from the initial plasma and started to propagate freely, the anisotropy became Σ_2. Indeed, this is very plausible if these anisotropies are kept small. Since we get $b \approx 0$ from the limiting case (29), we conclude that the anisotropy left that epoch almost with the same magnitude it entered there.

Since we have got little information on the vanishing of b, we might go deeper into its analysis and make it from the scratch. So, setting $\alpha = \pi/6$, for the sake of simplicity, and using the integral (28), we get

$$b = \frac{\Sigma_1 \Sigma_2 \ln(\Sigma_2/\Sigma_1)}{\Sigma_2 - \Sigma_1 + \Delta}, \tag{36}$$

where

$$\Delta = \Sigma_1 \Sigma_2 \ln \sqrt{\left(\frac{1+\Sigma_2}{1+\Sigma_1}\right)\left(\frac{1-\Sigma_1}{1-\Sigma_2}\right)}. \tag{37}$$

As we let the universe to expand N e-folds during this epoch, $\ln(a_2/a_1) = N$, we get $\ln(\Sigma_2/\Sigma_1) = Nb$. Hence, as we note that $\Sigma_1 < \Sigma_2$ implies $\Delta > 0$, we obtain

$$\frac{\Sigma_2 - \Sigma_1}{\Sigma_1} \leq \frac{\Sigma_2 - \Sigma_1}{\Sigma_1 \Sigma_2} < N, \tag{38}$$

that is,

$$\Sigma_1 < \Sigma_2 < (N+1)\Sigma_1, \tag{39}$$

which means that $b < [\ln(N+1)]/N$. In other words, the change in the anisotropy magnitude along the radiation era, as the universe expands N e-folds, is not greater than $\Sigma_2 \approx (N+1)\Sigma_1$.

5.2.4 From radiation-like to stiff-matter-like periods

In the isotropic model, the interval $1/3 < \mathrm{w} \leq 1$ is a candidate for the epoch between the inflationary and the radiation eras at "ultrahigh" densities. It contains the limiting stiff matter condition ($\mathrm{w} = 1$), for which the sound propagation attains the speed of light [25,26]. Interestingly enough, our model has naturally separated this regime from the others. Indeed, it appears as the physically relevant interval for which the origin is an unstable equilibrium. Hence, the universe tends to anisotropize even for arbitrarily small and non-

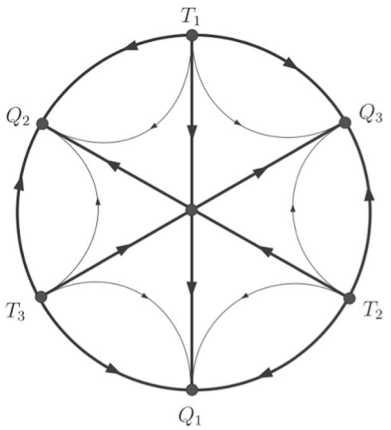

Fig. 4 The phase portrait in the Kasner disc ($\Sigma \leq 1$) for the radiation era ($\mathrm{w} = 1/3$). The solutions anisotropize towards the LRS models at the Q-Taub points, where $\Sigma = 1$, except the FLRW universe at the origin and those at the straight segment with $\alpha = \pi/2 + 2n\pi/3$

vanishing values of Σ. This is quite unexpected, for the tidal forces are still isotropic.

As we allow the equation of state to run from $\mathrm{w} = 1/3$ to $\mathrm{w} = 1$, the saddle-type equilibrium points $\widetilde{T}$'s appear at $\Sigma = (3\mathrm{w} - 1)/2$ and $\alpha = \pi/2 + 2(1-k)\pi/3$. In the late-time regime, the solutions approach the LRS universes at the Q-Taub points, with $\Sigma = 1$, except the isotropic model at the origin and those on the straight line connecting it to $\widetilde{T}$'s, for which $\Sigma \to (3\mathrm{w} - 1)/2$ as $a \to \infty$ (see Fig. 5).

The phase portrait in the Kasner disc for the stiff-matter-like situation is plotted in Fig. 6. In this case, the inner equilibrium points $\widetilde{T}$'s have coalesced with the T-Taub points so that any solution but the isotropic FLRW model at $\Sigma = 0$ tends to the maximum anisotropy $\Sigma \to 1$ at late-times.

From the formula (29), we get $b \approx (3\mathrm{w} - 1)/2$. This means that in the stiff-matter-like era, if there has been one, with $\mathrm{w} = 1$ and $b \approx 1$, have the universe passed through N e-folds during this high-density period, the anisotropy would increase just as well.

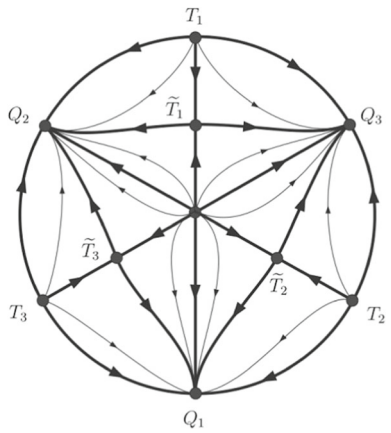

Fig. 5 The phase portrait in the Kasner disc ($\Sigma \leq 1$) for $1/3 < \mathrm{w} < 1$. Any solution but the FLRW universe at the center anisotropizes. In the late-time regime, they approach the LRS universes at the Q-Taub points, with $\Sigma = 1$. The only exceptions are in the lines $\alpha = \pi/2 + 2n\pi/3$, where $\Sigma \to (3\mathrm{w} - 1)/2$ as $a \to \infty$, the $\widetilde{T}$'s saddle-type equilibrium points

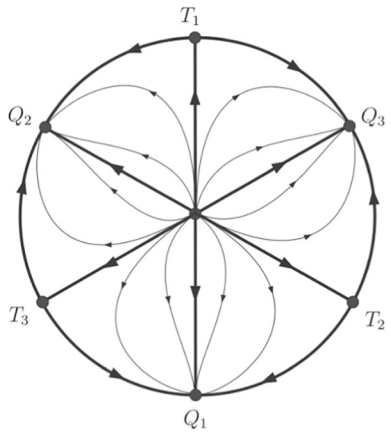

Fig. 6 The phase portrait in the Kasner disc ($\Sigma \leq 1$) for $\mathrm{w} = 1$. Any solution but the FLRW universe at the center anisotropizes to the borders of the Kasner disc ($\Sigma \to 1$ as $a \to \infty$). The saddle-type equilibrium points ($\widetilde{T}$'s) have coalesced with the T-Taub points at $\Sigma = 1$

6 Can the universe be anisotropic?

In this section, we use our findings to discuss anisotropy in the physical universe. Firstly, we analyze the no-hair argument for the elimination of any anisotropy in the Λ-dominated dynamics. We shall conclude that the universe hasn't existed long enough to see this mechanism working. In the sequence, we investigate whether the anisotropy in the Hubble parameter could be discarded using theoretical considerations. As we are going to see, there is no prior reason to underestimate it. In other words, its observational scrutiny is worth pursuing.

6.1 The epochs dominated by Λ and the "cosmic no-hair" argument

Let us first recover the cosmological constant in Einstein's equations, which we will assume to be positive, $\Lambda > 0$, and investigate how it would isotropize our spacetime, according to the "cosmic no-hair" theorem [22]. We can do it by substituting $\rho \to \rho + \Lambda$ and $\mathrm{P} \to \mathrm{P} - \Lambda$, which in our context is complemented as $\mathrm{P}_T \to \mathrm{P}_T - \Lambda$ and $\mathrm{P}_B \to \mathrm{P}_B$, that is, the pressure at the thermodynamic equilibrium is the carrier of the cosmological constant, while the bulk pressure, according to their definition in formula (12), remains unchanged. Therefore, the energy conservation (13) keeps the same form, but the generalized Friedmann equation (14) gains a supplementary term,

$$\mathrm{H}^2 = \Sigma^2 \mathrm{H}^2 + \frac{1}{T_0^2} + \frac{\rho}{3}, \tag{40}$$

where we have introduced the time parameter

$$T_0 = \sqrt{\frac{3}{\Lambda}} = \frac{1}{\Omega_\Lambda^{1/2}\,\mathrm{H}_0} \tag{41}$$

with Ω_Λ the ratio of the vacuum energy density at the instant $t = t_0$, as in the ΛCDM model [27]. In Eq. (15), there appears an extra term $-\Lambda/\mathrm{H}^2$ inside the first parentheses, which implies the substitution $\mathrm{w} \to (\mathrm{w} - \mathrm{w}_\Lambda(t))/(1 + \mathrm{w}_\Lambda(t))$ in (20), where $\mathrm{w}_\Lambda(t) = \Lambda/\rho(t)$. As we derive (40) and use (13) and (20) to replace $\dot{\rho}$ and $\dot{\Sigma}$, respectively, we arrive to the Raychaudhuri's equation,

$$\dot{\mathrm{H}} + \left(1 + 2\Sigma^2\right)\mathrm{H}^2 = -\frac{1}{6}\left(\rho + 3\mathrm{P} - 2\Lambda\right). \tag{42}$$

The strong energy hypothesis [28] in our restricted context implies $\rho \geq 0$ and $\rho + 3\mathrm{P} \geq 0$. As we assume an expanding scenario, $\mathrm{H} > 0$, it implies $\mathrm{H}T_0 \geq 1$, from (40), and $\dot{\mathrm{H}} + \mathrm{H}^2 \leq$

$\frac{1}{T_0^2}$, from (42). This is equivalent to $dx/(1-x^2) \leq dt/T_0$, with $x = \mathrm{H}T_0$. Integrating it from t_0 to $t_0 + \Delta t$, $\Delta t > 0$, we obtain

$$1 \leq \mathrm{H}T_0 \leq 1 + \frac{2\chi_0 e^{-2\Delta t/T_0}}{1 - \chi_0 e^{-2\Delta t/T_0}}, \tag{43}$$

where $\chi_0 = (\mathrm{H}_0 T_0 - 1)/(\mathrm{H}_0 T_0 + 1) > 0$. As we isolate Σ in (40), we obtain

$$\Sigma^2 \leq \frac{(\mathrm{H}T_0 - 1)(\mathrm{H}T_0 + 1)}{(\mathrm{H}T_0)^2}. \tag{44}$$

Using (43), which implies $1 + \mathrm{H}T_0 \leq 1 + \mathrm{H}_0 T_0$, and substituting T_0 as in (41), we obtain

$$\Sigma \leq \sqrt{\frac{1}{\Omega_\Lambda} - 1}\; e^{-\Omega_\Lambda \mathrm{H}_0 \Delta t}. \tag{45}$$

This is virtually the same argument used in [22], which shows that a positive cosmological constant leads the spacetime to exponentially approach an asymptotic isotropic state with a constant Hubble parameter. It works in the broader context of the Bianchi models, except for type IX. However, even if all the required hypotheses hold for the applicability of such an argument, the threshold of this isotropic universe is placed somewhere in time surpassing the age of the universe $\sim \mathrm{H}_0^{-1}$. For instance, if we take H_0 to be the value of the Hubble parameter at the moment in the late time universe when Λ begins to dominate, after a long period $\Delta t = \mathrm{H}_0^{-1}$, comparable to the age of the universe, we would have $\Sigma \lesssim 0.33$, for the current value of $\Omega_\Lambda \sim 0.7$. Therefore, this order of magnitude analysis shows us that this kind of argumentation is not enough, at least in our era, to discard anisotropy in the late time universe. In the best, the limits imposed by (45) would not give us any important information about the Hubble anisotropy but the fact that it is regular, that is, $\Sigma \leq 0.5$. But this should be quite expected from theoretical grounds, for otherwise, we could have a universe expanding in one direction while contracting in another one [21].

Undoubtedly, Wald's argument is very important to theoretical Cosmology, but it cannot be used to discard anisotropies in the Hubble sky, at least in our current era. On the other hand, since our model is much more restrictive, we can gain much more information about the behavior of Σ. Here, the Λ era would be represented by the regime where P_T gets closer to $-\rho$. This can be illustrated by setting w constant and near -1, just as in Sect. 5.2.1, where $-1 \leq \mathrm{w} < -1/3$. As we have shown, at that point the universe would commence a strong isotropization process, with $\Sigma \sim a^{-2}$ decreasing twice as fast as its expansion rate, as $\mathrm{w} \approx -1$ ($b \approx 2$), or just as its expansion rate, $\Sigma \sim a^{-1}$ as $\mathrm{w} \approx -1/3$. In any of these cases, the only possible behavior is isotropization, as can be seen in the global dynamics in the Kasner disc represented in Fig. 2. There are two important eras where that could have occurred: in the very early and in the late-time universes.

For the very early universe, our model has much more to tell about the inflationary than the BKL scenario. The reason for this is simple: while the first is highly compatible with the hypothesis of isotropic tidal forces, the chaotic behavior of the second would hardly let this characteristic be attained. Hence, as far as we assume that inflation took place, the energy-momentum tensor for the scalar field driving it would dominate the energy density and pressure in the universe, so that $\mathrm{P}_T \approx -\rho$. The universe would commence a strong isotropization process, with $\Sigma \sim a^{-2}$ decreasing twice as fast as its expansion rate ($b \approx 2$). At the end of this era, when $\mathrm{w} \sim -1/3$ [29], the (pre)reheating epoch would have begun, with $-1/3 \leq \mathrm{w} \leq 1$. As we put the e-fold duration of inflation and reheating as N_{inf} and N_{rh}, with $\mathrm{w} = -1$ and $\mathrm{w} = 1$, respectively, we would have an estimate for the net decrease of the anisotropy as e^{-N}, where $N \sim 2N_{inf} - N_{rh}$, according to our analysis following the formula (29). Recent estimates point to $N_{inf} \sim N_{rh} \sim 60$ [23,29]. This would lead the anisotropy still insignificant to be detected in the late-time sky, for the periods coming afterward which are dominated by radiation (anisotropization with $b \approx 0$), dust (isotropization with $b \approx 1/2$) and dark energy (isotropization with $b \approx 2$), would not last long enough to significantly change this tiny scale. In other words, as far as the universe could be considered spatially homogeneous on large scales, the existence of a mechanism like inflation, or any other that endures as long as it does and that violates the energy condition $\rho + 3\mathrm{P}_T > 0$, would put the Hubble anisotropy down to an insignificant role in the cosmic history.

6.2 Is it possible to exist a detectable Hubble anisotropy in the late-time universe?

As we have seen, there is no room for the Hubble anisotropy inside the inflationary ΛCDM environment. However, the arguments put forth should be valid as far as the inhomogeneities of the real universe do not hit the breaking point where the linear perturbations of the FLRW spacetimes are no longer valid [30,31]. If that happened, for instance, during the epoch of the formation of some structures (see section 12.3.7 in [23]), there would be no reason, a priory, to think that Σ would keep its tiny magnitude inherited from earlier epochs. The fact is that the success of the standard model of Cosmology should not prevent further scrutiny of its own tenets. Hence, it is fair to ask, whether from the observational viewpoint or a different theoretical perspective, about the possibility of detection of a significant Hubble anisotropy in the late-time universe.

On observational grounds, there is a growing debate concerning the order of magnitude of the variation of H_0 along the different directions in the cosmic sky [1–4,8].

In Ref. [10], the reader will find a complete and up-to-date manuscript considering the many observational aspects linked to anisotropy in Cosmology. Besides that, theoretical developments have appeared in order to clarify the patterns an anisotropic H_0 would have left in the sky, if any at all [32].

From the point of view of the results we have obtained so far in this manuscript, there are some significant conceptual considerations to add in favor of further scrutiny of the Hubble isotropy. First of all, we kept ourselves as close as we could get to the most reliable ΛCDM scenario, except for the nonlinear considerations on the anisotropy of the Hubble parameter: there are no inhomogeneities, for the model is spatially flat, the expansion is adiabatic and the "gravitational forces" acting on the free-falling observers are everywhere isotropic. Hence, our model could be seen as an arena to gain some knowledge of the behavior of Σ beyond the regime of linear perturbations, while other parameters responsible for linear corrections to the FLRW universe, typical of the perturbations in the ΛCDM environment, are neglected. As we have seen, even under these considerations, we have observed a tendency for the growth of the anisotropy, which is more stringent as far as we approach the values $w \geq 1/3$, which we have considered in Sects. 5.2.3 and 5.2.4 (see Figs. 4, 5, 6).

Let us work with the hypothesis that a significant Hubble anisotropy is confirmed in the late universe [8,10]. That would imply the failure of the linear perturbations of the ΛCDM model in describing the universe, at least at some moment in time. The issue of where it could have come from is harder to grasp and out of the scope of this manuscript. Let us just assume that, somehow, in a moment between the end of the radiation era and the beginning of the late-time Λ-dominated period, the Hubble anisotropy had a value Σ_{initial} many orders of magnitude greater than its counterpart predicted in the ΛCDM scenario. Our findings left us with many possibilities for theoretical speculations. For instance, the anisotropy could increase as $\Sigma \sim \ln a$, in the radiation-like regime ($w \approx 1/3$), or even, and less likely, as $\Sigma \sim a$, when the effective equation of state could be considered as high as $w \approx 1$. In any of these cases, the qualitative behaviors shown in Figs. 4, 5 and 6 tell us that the asymptotic growth of anisotropy is virtually the sole possibility. On the other hand, w soon starts to change towards the complete dominance of dark energy, at $w = -1$. During this process, the anisotropy can still increase, depending on where it is placed in the Kasner disc when $-1/3 < w < 1/3$. Figure 3 shows us two different behaviors at that epoch, isotropization and anisotropization, depending on where Σ is placed, in the innermost or outermost region in the Kasner disc, respectively. At some moment, it seems to be most likely that it started to decrease and has done so ever since. The very interesting aspect is that the Hubble anisotropy would fall off much slower than a^{-3}, that is, much slower than any other physical component of the universe, as the baryonic mass density ($\sim a^{-3}$) or the radiation energy density ($\sim a^{-4}$), according to the ΛCDM perspective [27], except for the constant vacuum energy density, represented by Λ. The decrease rate at $w = -1/3$ is just $\Sigma \sim a^{-1}$, while at $w = -1$ we have $\Sigma \sim a^{-2}$. Therefore, even if Σ_{initial} was not too large, its magnitude would not have decreased substantially ever since. This is a strong theoretical argument to justify the efforts for better observational scrutiny of the Hubble isotropy hypothesis.

7 Final remarks

In this manuscript, we have analyzed the spatially flat spacetimes under adiabatic expansion and isotropic tidal forces. The total pressure has naturally been divided into the equilibrium (P_T) and bulk (P_B) components, the first emulating its isotropic counterpart while the other exists due to anisotropic effects. We analyzed the dynamics of the Hubble anisotropy in the Kasner disc during the different epochs when the ratio $w = P_T/\rho$ could be held constant. The final framework is a simple and physically relevant scenario where the anisotropy can be understood in its fully non-linear aspects, which was dully depicted in the Kasner disc. For instance, the reader can have a glimpse of the overall aspects of the system and how it changes with w just by passing from Figs. 2, 3, 4, 5 and Fig. 6, from the isotropizing environment with $w = -1$ (Fig. 2) to the completely anisotropizing dynamics with $w = 1$ (Fig. 6).

Despite the many successes of the standard model of Cosmology, the isotropy hypothesis for the observed H_0 has been the subject of growing debate in the scientific community (see [10] and the references therein). From the theoretical point of view, new perspectives should appear as well, whether for supporting the observed data or to clarify the whole picture before our eyes. Here we have presented one possibility, very close to the ΛCDM picture, but sufficiently different from it to show the subtleties in the behavior of the anisotropy. As we have shown in Sect. 6, our model also justifies why the search for observational anisotropies in the Hubble parameter is worth pursuing.

Acknowledgements FSD is partially supported by Fundação de Amparo à Pesquisa do Estado de Minas Gerais—FAPEMIG [Grant number APQ-01158-17]. LFM is partially supported by Fundação de Amparo à Pesquisa do Estado de Minas Gerais—FAPEMIG [Grant number APQ-01105-18] and by Conselho Nacional de Desenvolvimento Científico e Tecnológico—CNPq [Grant number 311921/2020-5].

Data availability statement This manuscript has no associated data or the data will not be deposited. [Authors' comment: This manuscript is a theoretical investigation. No data repository has been used or created.]

Funded by SCOAP^3. SCOAP^3 supports the goals of the International Year of Basic Sciences for Sustainable Development.

References

1. T. Schucker, A. Tilquin, G. Valent, Bianchi I meets the Hubble diagram. Mon. Not. R. Astron. Soc. **444**(3), 2820–2836 (2014). https://doi.org/10.1093/mnras/stu1656. arXiv:1405.6523 [astro-ph.CO]
2. D. Zhao, J.-Q. Xia, Testing cosmic anisotropy with the E_p-E_{iso} ('Amati') correlation of GRBs. Mon. Not. R. Astron. Soc. **511**(4), 5661–5671 (2022). https://doi.org/10.1093/mnras/stac498
3. J. Soltis, A. Farahi, D. Huterer, C.M. Liberato, Percent-level test of isotropic expansion using type ia supernovae. Phys. Rev. Lett. **122**, 091301 (2019). https://doi.org/10.1103/PhysRevLett.122.091301
4. O. Akarsu, S. Kumar, S. Sharma, L. Tedesco, Constraints on a Bianchi type I spacetime extension of the standard ΛCDM model. Phys. Rev. D **100**(2), 023532 (2019). https://doi.org/10.1103/PhysRevD.100.023532. arXiv:1905.06949 [astro-ph.CO]
5. D. Saadeh, S.M. Feeney, A. Pontzen, H.V. Peiris, J.D. McEwen, How isotropic is the universe? Phys. Rev. Lett. **117**, 131302 (2016). https://doi.org/10.1103/PhysRevLett.117.131302
6. Planck Collaboration, Y. Akrami, M. Ashdown, J. Aumont, C. Baccigalupi, M. Ballardini, A. J. Banday, R. B. Barreiro, N. Bartolo, S. Basak, K. Benabed, M. Bersanelli, P. Bielewicz, J. J. Bock, J. R. Bond, J. Borrill, F. R. Bouchet, F. Boulanger, M. Bucher, C. Burigana, R. C. Butler, E. Calabrese, J.-F. Cardoso, B. Casaponsa, H. C. Chiang, L. P. L. Colombo, C. Combet, D. Contreras, B. P. Crill, P. de Bernardis, G. de Zotti, J. Delabrouille, J.-M. Delouis, E. Di Valentino, J. M. Diego, O. Doré, M. Douspis, A. Ducout, X. Dupac, G. Efstathiou, F. Elsner, T. A. Enßlin, H. K. Eriksen, Y., Fantaye, R. Fernandez-Cobos, F. Finelli, M. Frailis, A. A. Fraisse, E. Franceschi, A. Frolov, S. Galeotta, S. Galli, K. Ganga, R. T. Génova-Santos, M. Gerbino, T. Ghosh, J. González-Nuevo, K. M. Górski, A. Gruppuso, J. E. Gudmundsson, J. Hamann, W. Handley, F. K. Hansen, D. Herranz, E. Hivon, Z. Huang, A. H. Jaffe, W. C. Jones, E. Keihänen, R. Keskitalo, K. Kiiveri, J. Kim, N. Krachmalnicoff, M. Kunz, H. Kurki-Suonio, G. Lagache, J.-M. Lamarre, A. Lasenby, M. Lattanzi, C. R. Lawrence, M. Le Jeune, F. Levrier, M. Liguori, P. B. Lilje, V. Lindholm, M. López-Caniego, Y.-Z. Ma, J. F. Macías-Pérez, G. Maggio, D. Maino, N. Mandolesi, A. Mangilli, A. Marcos-Caballero, M. Maris, P. G. Martin, E. Martínez-González, S. Matarrese, N. Mauri, J. D. McEwen, P. R. Meinhold, A. Mennella, M. Migliaccio, M.-A. Miville-Deschênes, D. Molinari, A. Moneti, L. Montier, G. Morgante, A. Moss, P. Natoli, L. Pagano, D. Paoletti, B. Partridge, F. Perrotta, V. Pettorino, F. Piacentini, G. Polenta, J.-L. Puget, J. P. Rachen, M. Reinecke, M. Remazeilles, A. Renzi, G. Rocha, C. Rosset, G. Roudier, J. A. Rubiño-Martín, B. Ruiz-Granados, L. Salvati, M. Savelainen, D. Scott, E. P. S. Shellard, C. Sirignano, R. Sunyaev, A.-S. Suur-Uski, J. A. Tauber, D. Tavagnacco, M. Tenti, L. Toffolatti, M. Tomasi, T. Trombetti, L. Valenziano, J. Valiviita, B. Van Tent, P. Vielva, F. Villa, N. Vittorio, B. D. Wandelt, I. K. Wehus, A. Zacchei, J. P. Zibin, A. Zonca, Planck 2018 results—vii. Isotropy and statistics of the cmb. A&A **641**, 7 (2020). https://doi.org/10.1051/0004-6361/201935201
7. C.A.P. Bengaly, R. Maartens, N. Randriamiarinarivo, A. Baloyi, Testing the cosmological principle in the radio sky. J. Cosmol. Astropart. Phys. **2019**(09), 025–025 (2019). https://doi.org/10.1088/1475-7516/2019/09/025
8. P. Fosalba, E. Gaztanaga, Explaining cosmological anisotropy: evidence for causal horizons from CMB data (2020). https://doi.org/10.1093/mnras/stab1193. arXiv:2011.00910 [astro-ph.CO]
9. S. Yeung, M.-C. Chu, Directional variations of cosmological parameters from the Planck CMB data. Phys. Rev. D **105**(8), 083508 (2022). https://doi.org/10.1103/PhysRevD.105.083508. arXiv:2201.03799 [astro-ph.CO]
10. P.K. Aluri, et al. Is the observable universe consistent with the cosmological principle? (2022). arXiv:2207.05765 [astro-ph.CO]
11. C.B. Collins, S.W. Hawking, Why is the universe isotropic? Astrophys. J. **180**, 317–334 (1973). https://doi.org/10.1086/151965
12. V.A. Belinskii, I.M. Khalatnikov, E.M. Lifshitz, A general solution of the Einstein equations with a time singularity. Adv. Phys. **31**(6), 639–667 (1982). https://doi.org/10.1080/00018738200101428
13. C.W. Misner, Neutrino viscosity and the isotropy of primordial blackbody radiation. Phys. Rev. Lett. **19**, 533–535 (1967). https://doi.org/10.1103/PhysRevLett.19.533
14. C.W. Misner, The isotropy of the universe. Astrophys. J. **151**, 431 (1968). https://doi.org/10.1086/149448
15. J.D. Barrow, The isotropy of the universe. QJRAS **23**, 344 (1982)
16. B.K. Berger, in *Singularities in Cosmological Spacetimes*. ed. by A. Ashtekar, V. Petkov (Springer, Berlin, 2014), pp.437–460
17. V.G. LeBlanc, Asymptotic states of magnetic Bianchi i cosmologies. Class. Quantum Gravity **14**(8), 2281–2301 (1997). https://doi.org/10.1088/0264-9381/14/8/025
18. S. Calogero, J.M. Heinzle, Dynamics of Bianchi type I solutions of the Einstein equations with anisotropic matter. Annales Henri Poincare **10**, 225–274 (2009). https://doi.org/10.1007/s00023-009-0407-y. arXiv:0809.1008 [gr-qc]
19. E. Bittencourt, L.G. Gomes, R. Klippert, Bianchi-i cosmology from causal thermodynamics. Class. Quantum Gravity **34**(4), 045010 (2017). https://doi.org/10.1088/1361-6382/aa5994
20. B.B. Bizarria, G.A.S. Silva, L.G. Gomes, W.O. Clavijo, The oscillatory anisotropy in the spatially flat cosmological models. Ann. Phys. **432**, 168571 (2021). https://doi.org/10.1016/j.aop.2021.168571
21. F.S. Dias, G.B. Santos, L.G. Gomes, L.F. Mello, The power-law dependence between the matter-radiation and Hubble anisotropies. Int. J. Mod. Phys. D **31**(07), 2250049 (2022). https://doi.org/10.1142/S0218271822500493
22. R.M. Wald, Asymptotic behavior of homogeneous cosmological models in the presence of a positive cosmological constant. Phys. Rev. D **28**, 2118–2120 (1983). https://doi.org/10.1103/PhysRevD.28.2118
23. G.F.R. Ellis, R. Maartens, M.A.H. MacCallum, *Relativistic Cosmology* (Cambridge University Press, Cambridge, 2012)
24. F. Dumortier, J. Llibre, J. Artés, *Qualitative Theory Of Planar Differential Systems* (Springer, Berlin, 2007)
25. B.Z. Ya, The equation of state at ultrahigh densities and its relativistic limitations. J. Exp. Theor. Phys. **14**(05), 1143 (1962)
26. P.-H. Chavanis, Cosmology with a stiff matter era. Phys. Rev. D **92**, 103004 (2015). https://doi.org/10.1103/PhysRevD.92.103004
27. S. Weinberg, *Cosmology* (Oxford University Press, Oxford, 2008)
28. S.W. Hawking, G.F.R. Ellis, *The Large Scale Structure of Space-Time. Cambridge Monographs on Mathematical Physics* (Cambridge University Press, Cambridge, 1973). https://doi.org/10.1017/CBO9780511524646
29. H. Zhou, Q. Yu, Y. Pan, R. Zhou, W. Cheng, Reheating constraints on modified single-field natural inflation models.

Eur. Phys. J. C **82**(7), 588 (2022). https://doi.org/10.1140/epjc/s10052-022-10559-8. arXiv:2206.09892 [hep-ph]

30. T. Buchert, M. Carfora, G.F.R. Ellis, E.W. Kolb, M.A.H. MacCallum, J.J. Ostrowski, S. Räsänen, B.F. Roukema, L. Andersson, A.A. Coley, D.L. Wiltshire, Is there proof that backreaction of inhomogeneities is irrelevant in cosmology? Class. Quantum Gravity **32**(21), 215021 (2015). https://doi.org/10.1088/0264-9381/32/21/215021
31. S.R. Green, R.M. Wald, Comments on backreaction. (2015). arXiv:1506.06452 [gr-qc]
32. L.G. Gomes, The nonlinear patterns of the cosmic anisotropy: the spatially flat perfect fluid universes. Class. Quantum Gravity **39**(2), 027001 (2022). https://doi.org/10.1088/1361-6382/ac3ae1